Metalloporphyrin π-Cation Radicals. Molecular Structure and Spin Coupling in a Vanadyl Octaethylporphyrinate Derivative. An Unexpected Spin Coupling Path

Charles E. Schulz,*[1a] Hungsun Song,[1b] Young Ja Lee,[1b] Jalal U. Mondal,[1b,c] K. Mohanrao,[1b] Christopher A. Reed,*[1d] F. Ann Walker,*[1e] and W. Robert Scheidt*[1b]

Contribution from the Department of Physics, Knox College, Galesburg, Illinois 61401, Department of Chemistry and Biochemistry, University of Notre Dame, Notre Dame, Indiana 46556, Department of Chemistry, University of Southern California, Los Angeles, California 90089-0744, and Department of Chemistry and Biochemistry, San Francisco State University, San Francisco, California 94132

Received April 4, 1994[⊗]

Abstract: The preparation and characterization of a π-cation radical derivative of a vanadyl porphyrinate is described. $[VO(OH_2)(OEP^{\bullet})]SbCl_6$ is prepared by chemical oxidation of [VO(OEP)]; the formulation has been confirmed by a single-crystal X-ray structure determination. The coordinated water molecule of the unusual six-coordinate vanadyl complex is derived from solvent. Axial bond distances are the following: V–O = 1.578(4) Å and V–O(H_2O) = 2.473(8) Å; the vanadyl ion is displaced 0.46 Å from the 24-atom mean plane. The average V–N_p distance is 2.063 Å. Crystal data: a = 15.530(2) Å, b = 14.586(4) Å, c = 18.965(3) Å, and β = 106.20(1)°, monoclinic, space group $P2_1/n$, V = 4125.4 Å^3, Z = 4, $[VO_2N_4C_{36}H_{45}]SbCl_6$, R_1 = 0.053 and R_2 = 0.064 for 4707 observed data. EPR spectra have been measured for $[VO(OH_2)(OEP^{\bullet})]SbCl_6$ in the solid (powder) state, in a single crystal, and in fluid and frozen solution. The solution-state EPR spectra of $[VO(OH_2)(OEP^{\bullet})]SbCl_6$ are quite distinct, with vanadium hyperfine lines and with differing spectra in fluid and frozen solution. These solution spectra are identical to those reported earlier by others. In the solid state, the EPR spectrum of a polycrystalline sample consists of a single broad line with g = 1.99; single-crystal spectra also show vanadium hyperfine-splitting consistent with V–V coupling. The solid-state EPR intensity increases with increasing temperature. $[VO(OH_2)(OEP^{\bullet})]SbCl_6$ has also been characterized by a detailed temperature-dependent (6–300 K) magnetic susceptibility study. Satisfactory fits of the temperature-dependent moments are obtained from a model in which the vanadyl electron is ferromagnetically coupled to the porphyrin cation electron (J_{v-r} = 63 cm^{-1}) and two radical spins are antiferromagnetically coupled (J_{r-r} = −139 cm^{-1}). This model also gives a satisfactory prediction of all solid-state EPR properties. The intramolecular ferromagnetic coupling is consistent with the principle of cospatial, orthogonal magnetic orbitals. The intermolecular antiferromagnetic coupling appears to arise from a novel, steplike orientation of pairs of (OEP•) radicals.

Porphyrin π-cation radicals have played an important role in defining the principles of spin coupling in bioinorganic chemistry.[2] In earlier work,[3-8] we have investigated the notable differences in spin coupling between metal and porphyrin spins in a variety of derivatives that differ in metal ion, axial ligation, and/or porphyrin ligand. Both intra- and intermolecular spin-coupling can be significant. Two distinct intramolecular coupling mechanisms are found: (i) ferromagnetic coupling between the metal and ligand magnetic centers, leading to maximal spin multiplicity, and (ii) antiferromagnetic coupling, leading to a lower multiplicity state. It is found that case i is observed when the porphyrin radical is in an essentially planar environment that approximates D_{4h} symmetry. In this symmetry, the partially filled metal orbitals and the porphyrin π-radical orbital are orthogonal. Cospatiality leads to Hund's rule-like spin multiplicity. Case ii arises in lower symmetry systems where the metal and ligand magnetic orbitals are not strictly forbidden by symmetry from net overlap. The copper(II) π-cation radicals of TPP[4,9] and TMP,[7] which are S = 0 and 1 species, respectively, nicely illustrate these important core conformation effects on magnetic coupling. In well-characterized systems that display *inter*molecular coupling, it is the unpaired electrons on the porphyrin rings that are coupled. The magnitude of the coupling ranges from J = −14.7 cm^{-1} in one crystalline form of weakly coupled $[Zn(TPP^{\bullet})(OClO_3)]$ dimers to greater than −200 cm^{-1} in the strongly coupled (diamagnetic) novel dimer $[Zn(OEP^{\bullet})(OH_2)]_2(ClO_4)_2$.[6]

Cases where both intra- and intermolecular coupling are significant are less well-characterized. To date, the apparent requirements for such coupled radical systems would be a four- or five-coordinate metalloporphyrin radical in which the metal ion is paramagnetic and the porphyrin has modest steric constraints. However, $[Cu(OEP^{\bullet})]^+$ and $[Cu(OEC^{\bullet})]^+$ exhibit Cu–Cu triplet EPR spectra[10] with no evidence for unpaired radical electrons in either the EPR[10] or bulk magnetic susceptibility.[11] In the $[Fe(OEP^{\bullet})(Cl)]_2(ClO_4)_2$ dimer,[8] two different coupling

⊗ Abstract published in *Advance ACS Abstracts*, July 1, 1994.

(1) (a) Knox College. (b) University of Notre Dame. (c) Present address: Department of Chemistry, University of Texas—Pan American. (d) University of Southern California. (e) San Francisco State University. Present address: Department of Chemistry, University of Arizona, Tucson, AZ 85721.

(2) Reed, C. A.; Orosz, R. D. In *Research Frontiers in Magnetochemistry*; O'Connor, C. J., Ed.; World Scientific: Singapore, 1993; pp 351-393.

(3) Gans, P.; Buisson, G.; Duée, E.; Marchon, J.-C.; Erler, B. S.; Scholz, W. F.; Reed, C. A. *J. Am. Chem. Soc.* **1986**, *108*, 1223.

(4) Erler, B. S.; Scholz, W. F.; Lee, Y. J.; Scheidt, W. R.; Reed, C. A. *J. Am. Chem. Soc.* **1987**, *109*, 2644.

(5) Song, H.; Rath, N. P.; Reed, C. A.; Scheidt, W. R. *Inorg. Chem.* **1989**, *28*, 1839.

(6) Song, H.; Reed, C. A.; Scheidt, W. R. *J. Am. Chem. Soc.* **1989**, *111*, 6867.

(7) (a) Song, H.; Reed, C. A.; Scheidt, W. R. *J. Am. Chem. Soc.* **1989**, *111*, 6865. (b) Song, H.; Orosz, R. D.; Reed, C. A.; Scheidt, W. R. *Inorg. Chem.* **1990**, *29*, 4274.

(8) Scheidt, W. R.; Song, H.; Haller, K. J.; Safo, M. K.; Orosz, R. D.; Reed, C. A.; Debrunner, P. G.; Schulz, C. E. *Inorg. Chem.* **1992**, *31*, 939.

(9) Abbreviations used: TMP, dianion of tetramesitylporphyrin; TPP, dianion of tetraphenylporphyrin; OEP, dianion of octaethylporphyrin.

(10) Mengerson, C.; Subramanian, J.; Fuhrhop, J.-H. *Mol. Phys.* **1976**, *32*, 1299.

(11) The 6–300 K magnetic susceptibility data for $[Cu(OEP^{\bullet})]SbCl_6$ are cleanly fit by the Bleaney–Bowers model as a pair of weakly interacting Cu(II) ions with no residual magnetism attributable to the radical spins: Mondal, J. U.; Scheidt, W. R. Unpublished results.

0002-7863/94/1516-7196$04.50/0 © 1994 American Chemical Society

models with significantly different intermolecular coupling constants were found to provide adequate fits of the Mössbauer and magnetic susceptibility data. Vanadyl porphyrinates would appear to be ideally simple systems that could provide quantitative characterization of the combined effects of intra- and intermolecular spin coupling.

Previous reports of magnetic properties of vanadyl porphyrin π-cation radicals are somewhat divergent. Reported solution EPR spectra of $[VO(OEP^{\bullet})]^+$ are consistent only with dimer formation (with quenching of the radical π-electrons) at low (80 K) temperature[12] and an intramolecular, ferromagnetic, monomeric triplet at room temperature.[13] The room temperature magnetic susceptibility data for $[VO(TPP^{\bullet})]^+$ have been interpreted as a ferromagnetic coupling of the radical spin with the vanadyl d_{xy} electron (which is orthogonal to the radical orbital if the molecule has local C_{4v} symmetry).[4] However, the significance of these assignments remains somewhat tenuous in the absence of detailed structural information. As we have noted in previous investigations of magnetically interesting compounds, we emphasize susceptibility measurements on analytically pure solids since such measurements are most accurately made for solids. We also attempt to prepare single-crystal samples for X-ray structure analysis and to prepare adequate amounts of such crystalline samples of definite phase so that all measurements can be assessed in terms of known molecular structure and conformation and with well-defined intermolecular interactions. The preparation of appropriate crystalline samples of porphyrin π-cation radicals has turned out to be a substantial challenge. Crystals adequate for single crystal structure determinations have proven quite elusive, especially those of octaethylporphyrin derivatives.

In this paper we describe the preparation and characterization of a vanadyl octaethylporphyrin π-cation radical derivative. A crystal structure determination shows it to be $[VO(OH_2)(OEP^{\bullet})]SbCl_6$, a six-coordinate complex. The closest approach of vanadium(IV) ions in the lattice is 7.46 Å and π–π stacking is absent. This would seem to suggest that only monomeric models should be considered to explain the observed, temperature-dependent, solid-state magnetism. However, a dimeric model, in which there is intramolecular ferromagnetic magnetic coupling between a vanadyl d-electron and a π-cation radical and, at the same time, intermolecular ferromagnetic coupling between two cation radicals is required for consistency of the magnetic susceptibility and the EPR data. An unusual intermolecular coupling path is proposed.

Experimental Section

General. UV–vis spectra were recorded on a Perkin-Elmer Lambda 4C spectrometer and IR spectra on a Perkin-Elmer Model 883 spectrometer in KBr pellets prepared in the drybox. Magnetic measurements were performed on finely ground samples (0.030 g) in Al buckets on a SHE Model 905 SQUID susceptometer operating at 2 or 10 KG. Diamagnetic corrections were calculated from Pascal's constants and a value of -704×10^{-6} cgs for H_2OEP was used.[14] EPR spectra were obtained at 77 K and/or <30 K with a Varian E-12 spectrometer operating at X-band and equipped with Varian flowing nitrogen and Air Products helium variable temperature controllers. Single-crystal measurements were made on a Bruker X-band EPR spectrometer with an Oxford Instruments Helium Cryostat at the National EPR Center at Urbana. H_2OEP was purchased from Midcentury. Solvents were purified[15] by standard methods and stored over molecular sieves. Pure alkanes were purchased from Phillips Petroleum. Reactions were carried out under nitrogen or argon (H_2O < 10 ppm) in Schlenkware. All solid weightings and transfers were carried out in a Vacuum Atmospheres drybox.

Table 1. Crystallographic Data for $[VO(OEP^{\bullet})(H_2O)]SbCl_6$

$SbVCl_6O_2N_4C_{36}H_{46}$	mol wt = 952.2
a = 15.530(2) Å	space group = $P2_1/n$
b = 14.586(4) Å	T = 293 K
c = 18.965(3) Å	λ = 0.71073 Å
β = 106.20(1)°	μ = 1.305 mm^{-1}
V = 4125.4	R_1 = 0.053
Z = 4	R_2 = 0.064

Syntheses. (a) [VO(OEP)]. [VO(OEP)] was prepared[16] by reacting a pulverized mixture of 0.30 g (0.56 mmol) of H_2OEP and 0.98 g (2.81 mmol) of $V(acac)_3$ in a test tube. The tube was heated for 45 min at 240 °C in a mineral oil bath. The solid was dissolved in CH_2Cl_2 (100 mL) and filtered through a medium frit. The solution was chromatographed on a silica gel column (45 cm × 2.5 cm). The first fraction was collected and the CH_2Cl_2 solution evaporated. The resulting solid was recrystallized from benzene/methanol. λ_{max} (CH_2Cl_2) 570, 532, 407, and 328 nm. [VO(OEP)] was also prepared from $VO(SO_4)$ and H_2OEP in refluxing DMF.[17]

(b) $[VO(OH_2)(OEP^{\bullet})]SbCl_6$. [VO(OEP)] (96 mg, 0.16 mmol) and tris(4-bromophenyl)aminium hexachloroantimonate,[18] $(BrC_6H_4)_3NSbCl_6$ (196 mg, 0.24 mmol), were stirred overnight in dry dichloromethane (30 mL). The solution was filtered through a medium glass frit and dry heptane (30 mL) added. After 5 days, the solution was filtered and the microcrystalline solid washed with dry heptane. Yield 135 mg (91%). Crystals suitable for diffraction studies were prepared by dissolving 66 mg of $[VO_2N_4C_{36}H_{45}]SbCl_6$ in 12 mL of CH_2Cl_2 containing 20 mg of $(BrC_6H_4)_3NSbCl_6$. The solution was filtered and divided into two 10-mL beakers. One beaker was placed over heptane in a crystallizing jar and the other over dry nonane. The crystallizing jars were sealed and set aside. After 2 days, the solution placed over nonane had formed rectangular plates which were washed with hexane. The solution placed over heptane took several days longer to produce single crystals of similar shape. Both crystallizing procedures yield materials with identical diffraction patterns and identical UV–vis spectra. λ_{max} (CH_2Cl_2) 622, 515, 474 (sh), 391, 329 (sh) nm. A strong IR band at 1533 cm^{-1} was observed for samples of $[VO(OH_2)(OEP^{\bullet})]SbCl_6$ which was absent in [VO(OEP)], and the Sb–Cl stretch was observed at 342 cm^{-1}. All magnetic susceptibilities and other physical measurements were taken on crystalline specimens prepared in this fashion. Anal. Calcd for $[VO_2N_4C_{36}H_{45}]SbCl_6$: C, 45.41; H, 4.87; N, 5.88; Cl, 22.34. Found: C, 44.54; H, 4.76; N, 5.96; Cl, 22.79.

X-ray Structure Determination of $[VO(OH_2)(OEP^{\bullet})]SbCl_6$. Preliminary examination of a crystal obtained as above led to the assignment of a four-molecule monoclinic unit cell with the uniquely determined space group $P2_1/n$. Intensity data collection and final cell constants were obtained with a crystal specimen of dimensions 0.45 × 0.23 × 0.06 mm. All measurements were made on an Enraf-Nonius CAD4 diffractometer with Mo Kα radiation. Least-squares refinement of the setting angles of 25 automatically centered reflections with $22.4 \le 2\theta \le 27.4°$ led to the cell constants reported in Table 1. For a cell content of $4[VO_2N_4C_{36}H_{45}]SbCl_6$, the calculated density is 1.53 g/cm^3; the experimental density was 1.51 g/cm^3.

Intensity data were measured using graphite-monochromated Mo Kα radiation and θ–2θ scanning at the ambient laboratory temperature of 19 ± 1 °C. Three standard reflections were measured every hour as a monitor of the long-term stability of the experiment; no significant variation was observed. Intensity data were reduced and included an analytical correction[19] for absorption (μ = 13.05 cm^{-1}). A total of 4707 reflections having $\sin\theta/\lambda \le 0.649$ Å^{-1} and $F_o \ge 3.0\sigma(F_o)$ were taken as observed and used in the solution and refinement of the structure. The structure was solved using the direct methods program MULTAN.[20] The resulting E-map gave positions for all atoms except some of the peripheral ethyl group carbon atoms. The positions of these remaining atoms were readily

(12) Lemtur, A.; Chakravortay, K.; Dhar, T. K.; Subramanian, J. *J. Phys. Chem.* **1984**, *88*, 5603.
(13) Luckhurst, G. R.; Setaka, M.; Subramanian, J. *Mol. Phys.* **1976**, *32*, 1299. Subramanian, J. In *Porphyrins and Metalloporphyrins*; Smith, K. M., Ed.; Elsevier: Amsterdam, 1975; p 584.
(14) Eaton, S. S.; Eaton, G. R. *Inorg. Chem.* **1980**, *19*, 1095.
(15) Perrin, D. D.; Armarego, W. L. F.; Perrin, D. R. *Purification of Laboratory Chemicals*; Pergamon: New York, 1980.
(16) Buchler, J. W.; Eikelmann, G.; Puppe, L.; Rohbock, K.; Schneehage, H. H.; Weck, D. *Liebigs Ann. Chem.* **1971**, *745*, 135.
(17) Adler, A. D.; Longo, F. R.; Kampas, F.; Kim, J. *J. Inorg. Nucl. Chem.* **1970**, 2443.
(18) Bell, F. A.; Ledwirth, A.; Sherrington, D. C. *J. Chem. Soc. C* **1969**, 2719.
(19) Coppens, P. *Acta Crystallogr.* **1965**, *18*, 1035.

Table 2. Fractional Coordinates for $[VO(OEP^{\bullet})(H_2O)]SbCl_6$[a]

atom	x	y	z
Sb	0.458877(28)	0.26173(3)	0.87986(3)
Cl(1)	0.45553(21)	0.37318(20)	0.78800(18)
Cl(2)	0.50167(18)	0.38109(25)	0.96512(18)
Cl(3)	0.46201(18)	0.15087(28)	0.96793(21)
Cl(4)	0.61138(12)	0.23327(15)	0.89038(14)
Cl(5)	0.30854(13)	0.29150(18)	0.87444(18)
Cl(6)	0.41464(20)	0.15204(20)	0.78676(18)
V	0.02598(6)	0.24240(7)	0.06487(6)
V′	0.0446(23)	0.2529(24)	0.1232(23)
O	0.00087(28)	0.24114(29)	−0.02167(22)
O(w)	0.0684(5)	0.2488(6)	0.2005(4)
N(1)	−0.0686(3)	0.1547(3)	0.08501(27)
N(2)	−0.0504(3)	0.3504(3)	0.08446(27)
N(3)	0.1343(3)	0.3302(3)	0.09115(27)
N(4)	0.11620(29)	0.1355(3)	0.09065(28)
C(a1)	−0.0635(4)	0.0612(4)	0.0912(3)
C(a2)	−0.1561(4)	0.1776(4)	0.0809(3)
C(a3)	−0.1398(4)	0.3460(4)	0.0791(3)
C(a4)	−0.0279(4)	0.4410(4)	0.0907(3)
C(a5)	0.1328(4)	0.4244(4)	0.0977(3)
C(a6)	0.2190(3)	0.3091(4)	0.0895(3)
C(a7)	0.2032(4)	0.1396(4)	0.0902(3)
C(a8)	0.0969(4)	0.0442(4)	0.0964(3)
C(b1)	−0.1503(4)	0.0233(4)	0.0918(3)
C(b2)	−0.2070(4)	0.0948(4)	0.0859(3)
C(b3)	−0.1762(4)	0.4379(4)	0.0815(3)
C(b4)	−0.1075(4)	0.4970(4)	0.0883(3)
C(b5)	0.2210(4)	0.4623(4)	0.1023(3)
C(b6)	0.2741(4)	0.3922(4)	0.0956(3)
C(b7)	0.2415(4)	0.0478(4)	0.0938(4)
C(b8)	0.1755(4)	−0.0109(4)	0.0990(3)
C(m1)	0.0137(4)	0.0112(4)	0.0961(3)
C(m2)	−0.1887(4)	0.2659(4)	0.0755(3)
C(m3)	0.0568(4)	0.4753(4)	0.0970(3)
C(m4)	0.2498(4)	0.2202(4)	0.0854(3)
C(11)	−0.1677(4)	−0.0760(4)	0.1022(4)
C(12)	−0.1432(6)	−0.1023(5)	0.1814(5)
C(21)	−0.3029(4)	0.0951(4)	0.0861(4)
C(22)	−0.3161(5)	0.1221(7)	0.1595(5)
C(31)	−0.2718(4)	0.4585(4)	0.0765(4)
C(32)	−0.2947(5)	0.4437(6)	0.1479(4)
C(41)	−0.1068(4)	0.5983(4)	0.0946(4)
C(42)	−0.0708(6)	0.6320(6)	0.1721(5)
C(51)	0.2457(4)	0.5616(4)	0.1159(4)
C(52)	0.2688(6)	0.5871(5)	0.1958(4)
C(61)	0.3697(4)	0.3918(5)	0.0943(4)
C(62)	0.4352(5)	0.3666(7)	0.1651(5)
C(71)	0.3355(4)	0.0272(4)	0.0940(4)
C(72)	0.4028(5)	0.0418(6)	0.1672(5)
C(81)	0.1809(4)	−0.1130(4)	0.1076(4)
C(82)	0.1979(7)	−0.1441(6)	0.1858(5)

[a] The estimated standard deviations of the least significant digits are given in parentheses.

found in subsequent difference Fourier syntheses. During least-squares refinement a small amount of disorder involving the vanadium atom became apparent: a second, minor position of the vanadium atom (on the opposite side of the porphinato plane) was found. This minor component (V′) had an occupancy factor of 0.03(1); the major component was 0.97. Difference Fourier syntheses also provided evidence for most hydrogen atoms of the molecule. All hydrogen atoms of the molecule except those of the water ligand were idealized (C–H = 0.95 Å and B(H) = B(C) + 1.0 Å^2). This model was refined to convergence with anisotropic thermal parameters for all heavy atoms. At convergence, R_1 = 0.055 and R_2 = 0.067 with the error of fit equal to 1.93. At this point the question of whether the aquo ligand position was fully occupied was explored. Refinement of the occupancy factor for the aquo ligand converged at an occupancy factor of 0.60(2) and a more reasonable value for the thermal parameter of the oxygen atom. This model, at convergence, had R_1 = 0.053, R_2 = 0.064, and GOF = 1.84. It is not clear whether this refinement reflects a partial occupancy of water or a better fit to some small disorder in the aquo ligand position. In any event, the metrical details of the two refinements differed immaterially; the results of the second refinement are reported herein. The calculated density decreases to 1.52 g/cm^3 in satisfactory agreement with observation. A final difference Fourier map had peaks as large as 1.2 e/Å^3 near the hexachloroantimonate anion but was judged otherwise to be featureless. Final values of the atomic coordinates are given in Table 2. Values of anisotropic thermal parameters and fixed hydrogen atom positions are reported in Tables S2 and S3 of the supplementary material.

(20) Programs used in this study included local modifications of Main, Hull, Lessinger, Germain, Declerq, and Woolfson's MULTAN, Jacobson's ALLS, Zalkin's FORDAP, Busing and Levy's ORFFE and ORFLS, and Johnson's ORTEP2. Atomic form factors were from: Cromer, D. T.; Mann, J. B. *Acta Crystallogr., Sect. A* **1968**, *A24*, 321. Real and imaginary corrections for anomalous dispersion in the form factor of the vanadium and chlorine atoms were from: Cromer, D. T.; Liberman, D. J. *J. Chem. Phys.* **1970**, *53*, 1891. Scattering factors for hydrogen were from: Stewart, R. F.; Davidson, E. R.; Simpson, W. T. *J. Chem. Phys.* **1965**, *42*, 3175. All calculations were performed on a VAX 11/730 computer.

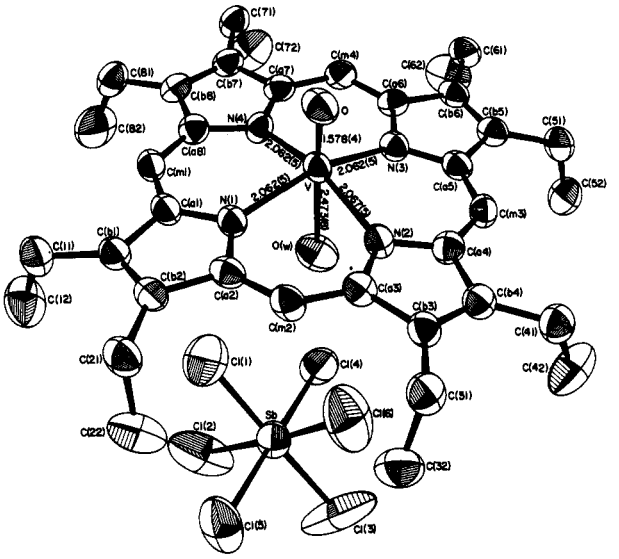

Figure 1. ORTEP diagram of $[VO(OH_2)(OEP^{\bullet})]SbCl_6$ displaying the atom labeling scheme used throughout the paper. Bond distances in the coordination group are shown. A spatially correct $SbCl_6^-$ ion is also shown in the figure.

Results

The π-cation radical $[VO(OH_2)(OEP^{\bullet})]SbCl_6$ has been characterized by IR and UV–vis spectroscopy, temperature-dependent solid-state magnetic susceptibilities, solution, powder, and single-crystal EPR, and a single-crystal X-ray structure determination. All data for this complex are consistent with the formulation of the complex as a ring-oxidized vanadyl porphyrin species. We attempted to similarly characterize $[VO(TPP^{\bullet})]SbCl_6$ and $[VO(TMP^{\bullet})]SbCl_6$. An X-ray structure or a single-crystal EPR determination of $[VO(TPP^{\bullet})]SbCl_6$ was not possible owing to our inability to obtain the needed single crystals, and the vanadyl TMP radical could not be obtained in a pure form. Since we have been unable to adequately define the solid-state structures of either of these latter species, they will not be discussed further in this paper.

The crystal structure determination of the π-cation derivative of [VO(OEP)] shows that it has the idealized composition of $[VO(OH_2)(OEP^{\bullet})]SbCl_6$. Thus the species is an apparent monomeric, six-coordinate complex with oxo and water as the axial ligands. The O–V–O angle is 178.14(24)°. The vanadium ion is displaced from the mean plane of the 24-atom porphinato core by 0.46 Å toward the axial oxo ligand. The V–O distances are 1.578(4) and 2.473(8) Å, while the average V–N_p bond distance is 2.063 Å. An overall view of the molecule is given in Figure 1, which also shows the atom labeling scheme and the bond distances within the coordination group of the cation. Also shown in Figure 1 is the hexachloroantimonate counterion in its correct spatial relationship to the vanadyl porphyrin cation. This hexachloroantimonate ion is the closest one to the illustrated vanadyl complex with a V···Sb distance of 6.34 Å. The vanadium

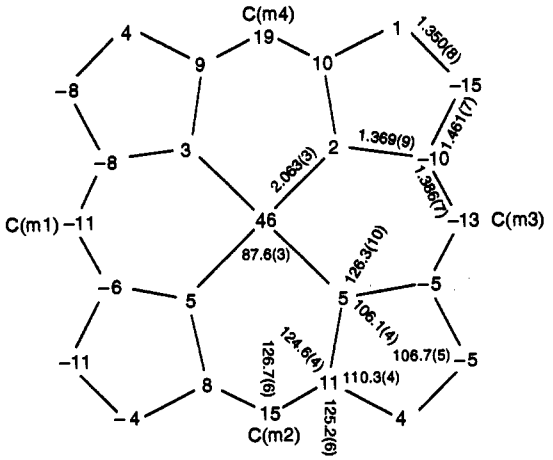

Figure 2. Formal diagram of the porphinato core in $[VO(OH_2)(OEP^{\bullet})]SbCl_6$ displaying the displacement, in units of 0.01 Å, from the mean plane of the porphinato core. Also displayed in the figure are the average bond distances and angles for the chemically unique parameters of the core.

Table 3. Bond Distances in $[VO(OEP^{\bullet})(H_2O)]SbCl_6$[a]

type	distances, Å	type	distances, Å
V–N(1)	2.062(5)	C(a6)–C(m4)	1.392(8)
V–N(2)	2.067(5)	C(a7)–C(b7)	1.459(8)
V–N(3)	2.062(5)	C(a7)–C(m4)	1.396(8)
V–N(4)	2.062(5)	C(a8)–C(b8)	1.451(8)
V–O	1.578(4)	C(a8)–C(m1)	1.378(8)
V–O(w)	2.473(8)	C(b1)–C(b2)	1.349(8)
V–V′	1.07(4)	C(b1)–C(11)	1.496(8)
V′–N(1)	2.23(4)	C(b2)–C(21)	1.489(8)
V′–N(2)	2.03(4)	C(b3)–C(b4)	1.349(8)
V′–N(3)	2.01(4)	C(b3)–C(31)	1.492(8)
V′–N(4)	2.22(4)	C(b4)–C(41)	1.483(8)
V′–O	2.65(4)	C(b5)–C(b6)	1.343(8)
V′–O(w)	1.41(4)	C(b5)–C(51)	1.503(9)
N(1)–C(a1)	1.369(7)	C(b6)–C(61)	1.491(8)
N(1)–C(a2)	1.379(7)	C(b7)–C(b8)	1.361(8)
N(2)–C(a3)	1.366(7)	C(b7)–C(71)	1.489(8)
N92)–C(a4)	1.364(8)	C(b8)–C(81)	1.479(9)
N93)–C(a5)	1.381(7)	C(11)–C(12)	1.493(10)
N(3)–C(a6)	1.359(7)	C(21)–C(22)	1.516(10)
N(4)–C(a7)	1.356(7)	C(31)–C(32)	1.508(9)
N(4)–C(a8)	1.375(7)	C(41)–C(42)	1.501(10)
C(a1)–C(b1)	1.460(7)	C(51)–C(52)	1.504(10)
C(a1)–C(m1)	1.384(8)	C(61)–C(62)	1.486(10)
C(a2)–C(b2)	1.461(8)	C(71)–C(72)	1.502(10)
C(a2)–C(m2)	1.377(8)	C(81)–C(82)	1.502(11)
C(a3)–C(b3)	1.459(8)	Sb–Cl(1)	2.373(3)
C(a3)–C(m2)	1.385(8)	Sb–Cl(2)	2.343(3)
C(a4)–C(b4)	1.472(8)	Sb–Cl(3)	2.316(3)
C(a4)–C(m3)	1.381(8)	Sb–Cl(4)	2.357(2)
C(a5)–C(b5)	1.457(8)	Sb–Cl(5)	2.349(2)
C(a5)–C(m3)	1.392(8)	Sb–Cl(6)	2.339(3)
C(a6)–C(b6)	1.470(8)		

[a] The numbers in parentheses are the estimated standard deviations. V′ refers to the disordered vanadium atom.

atoms appear well-separated in the crystal lattice with the closest V···V distances 7.46 and 7.88 Å.

Figure 2 is a formal drawing of the porphinato core in $[VO(OH_2)(OEP^{\bullet})]SbCl_6$ displaying the deviation of each atom (in units of 0.01 Å) from the mean plane of the core. Figure 2 also shows the averaged values of bond parameters in the core. The numbers in parentheses following each averaged value are the estimated standard deviations of the averaged value calculated on the assumption that the averaged values are all drawn from the same population. Individual values of bond distances and angles are given in Tables 3 and 4.

Experimental temperature-dependent magnetic susceptibility data for $[VO(OH_2)(OEP^{\bullet})]SbCl_6$ are shown in Figure 3. Data

Table 4. Bond Angles in $[VO(OEP^{\bullet})(H_2O)]SbCl_6$

type	angle, deg	type	angle, deg
N(1)VN(2)	88.01(18)	N(3)C(a5)C(m3)	124.5(5)
N(1)VN(3)	156.32(20)	C(b5)C(a5)C(m3)	125.4(6)
N(1)VN(4)	87.65(18)	N(3)C(a6)C(b6)	111.0(5)
N(1)VO	101.73(20)	N(3)C(a6)C(m4)	124.2(5)
N(1)VO(w)	80.07(23)	C(b6)C(a6)C(m4)	124.8(5)
N(2)VN(3)	87.35(19)	N(4)C(a7)C(b7)	110.7(5)
N(2)VN(4)	156.89(21)	N(4)C(a7)C(m4)	124.9(5)
N(2)VO	102.02(21)	C(b7)C(a7)C(m4)	124.4(5)
N(2)VO(w)	77.51(23)	N(4)C(a8)C(b8)	109.9(5)
N(3)VN(4)	87.57(18)	N(4)C(a8)C(m1)	124.3(5)
N(3)VO	101.95(20)	C(b8)C(a8)C(m1)	125.8(6)
N(3)VO(w)	76.25(23)	C(a1)C(b1)C(b2)	106.8(5)
N(4)VO	101.09(22)	C(a1)C(b1)C(11)	124.6(5)
N(4)VO(w)	79.39(24)	C(b2)C(b1)C(11)	128.4(5)
OVO(w)	178.14(24)	C(a2)C(b2)C(b1)	106.9(5)
N(1)V′N(2)	84.5(13)	C(a2)C(b2)C(21)	123.9(5)
N(1)V′N(3)	144.3(21)	C(b1)C(b2)C(21)	129.1(5)
N(1)V′N(4)	79.9(12)	C(a3)C(b3)C(b4)	106.8(5)
N(1)V′O	70.7(11)	C(a3)C(b3)C(31)	124.7(5)
N(1)V′O(w)	105.4(20)	C(b4)C(b3)C(31)	128.5(6)
N(2)V′N(3)	89.6(15)	C(a4)C(b4)C(b3)	106.4(5)
N(2)V′N(4)	143.9(21)	C(a4)C(b4)C(41)	124.3(5)
N(2)V′O	73.7(12)	C(b3)C(b4)C(41)	129.3(6)
N(2)V′O(w)	111.0(21)	C(a5)C(b5)C(b6)	107.4(5)
N(3)V′N(4)	84.6(13)	C(a5)C(b5)C(51)	124.5(6)
N(3)V′O	73.8(12)	C(b6)C(b5)C(51)	128.1(6)
N(3)V′O(w)	109.6(21)	C(a6)C(b6)C(65)	106.0(5)
N(4)V′O	70.4(11)	C(a6)C(b6)C(61)	123.9(6)
N(4)V′O(w)	104.5(20)	C(b5)C(b6)C(61)	130.2(6)
OV′O(w)	173.8(22)	C(a7)C(b7)C(b8)	106.0(5)
VN(1)C(a1)	127.3(4)	C(a7)C(b7)C(71)	124.9(5)
VN(1)C(a2)	125.5(4)	C(b8)C(b7)C(71)	129.1(6)
V′N(1)C(a1)	126.2(10)	C(a8)C(b8)C(b7)	107.0(5)
V′N(1)C(a2)	122.6(10)	C(a8)C(b8)C(81)	125.2(6)
C(a1)N(1)C(a2)	106.2(5)	C(b7)C(b8)C(81)	127.7(6)
VN(2)C(a3)	125.0(4)	C(a1)C(m1)C(a8)	127.5(6)
VN(2)C(a4)	127.5(4)	C(a2)C(m2)C(a3)	126.9(5)
V′N(2)C(a3)	127.9(10)	C(a4)C(m3)C(a5)	126.3(6)
V′N(2)C(a4)	120.3(11)	C(a6)C(m4)C(17)	126.1(5)
C(a3)N(2)C(a4)	106.3(5)	C(b1)C(11)C(12)	112.1(6)
VN(3)C(a5)	127.3(4)	C(b2)C(21)C(22)	113.2(6)
VN(3)C(a6)	125.7(4)	C(b3)C(31)C(32)	113.2(5)
V′N(3)C(a5)	119.9(11)	C(b4)C(41)C(42)	113.4(6)
V′N(3)C(a6)	129.5(11)	C(b5)C(51)C(52)	112.9(6)
C(a5)N(3)C(a6)	105.6(5)	C(b6)C(61)C(62)	114.8(6)
VN(4)C(a7)	125.3(4)	C(b7)C(71)C(72)	113.8(6)
VN(4)C(a8)	127.0(4)	C(b8)C(81)C(82)	113.3(6)
V′N(4)C(a7)	123.0(10)	Cl(1)SbCl(2)	86.64(13)
V′N(4)C(a8)	126.0(10)	Cl(1)SbCl(3)	178.95(15)
C(a7)N(4)C(a8)	106.4(5)	Cl(1)SbCl(4)	89.92(9)
N(1)C(a1)C(b1)	110.2(5)	Cl(1)SbCl(5)	91.33(11)
N(1)C(a1)C(m1)	124.0(5)	Cl(1)SbCl(6)	88.44(13)
C(b1)C(a1)C(m1)	125.7(5)	Cl(2)SbCl(3)	94.37(16)
N(1)C(a2)C(b2)	109.8(5)	Cl(2)SbCl(4)	89.29(9)
N(1)C(a2)C(m2)	124.5(5)	Cl(2)SbCl(5)	88.85(10)
C(b2)C(a2)C(m2)	125.6(5)	Cl(2)SbCl(6)	175.06(13)
N(2)C(a3)C(b3)	110.4(5)	Cl(3)SbCl(4)	89.86(9)
N(2)C(a3)C(m2)	125.1(5)	Cl(3)SbCl(5)	88.93(11)
C(b3)C(a3)C(m2)	124.5(5)	Cl(3)SbCl(6)	90.55(15)
N(2)C(a4)C(b4)	110.0(5)	Cl(4)SbCl(5)	177.69(10)
N(2)C(a4)C(m3)	125.0(5)	Cl(4)SbCl(6)	91.15(10)
C(b4)C(a4)C(m3)	125.0(6)	Cl(5)SbCl(6)	90.82(10)
N(3)C(a5)C(b5)	110.1(5)		

[a] The numbers in parentheses are the estimated standard deviations. V′ refers to the disordered vanadium atom.

for two independent preparations are illustrated and show the level of reproducibility of the magnetic susceptibility data for this compound. The unusual temperature dependence makes clear that any fit of the data will be complex; however, two models that provide quantitatively acceptable simulations of the magnetic data for $[VO(OH_2)(OEP^{\bullet})]SbCl_6$ have been obtained.

The first is a model in which the vanadyl electron is coupled to the porphyrin cation radical electron, i.e., a monomeric (intramolecular) coupling model. The 3d levels of the vanadyl

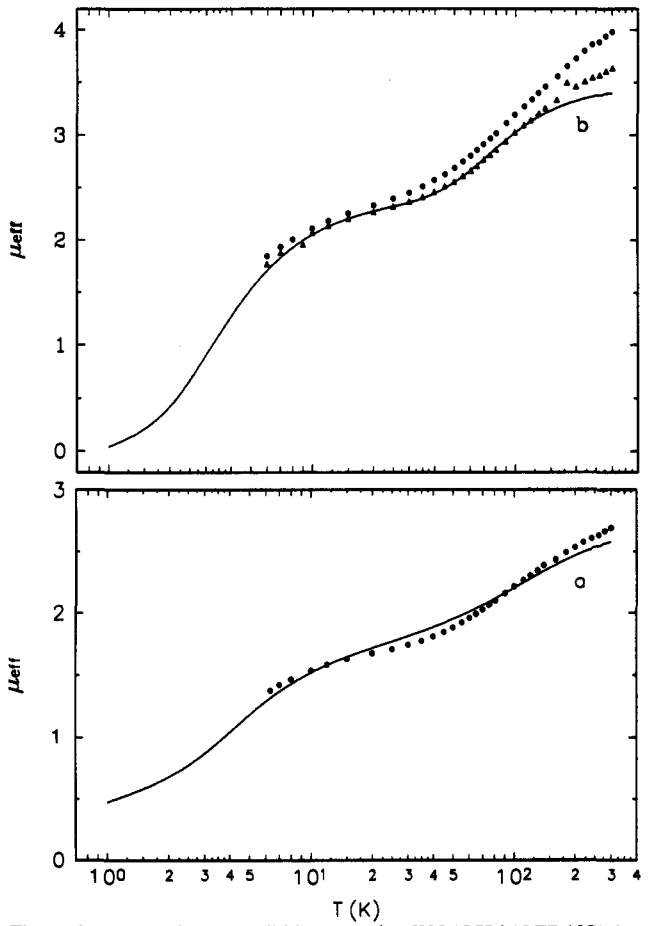

Figure 3. Magnetic susceptibility data for $[VO(OH_2)(OEP^{\bullet})]SbCl_6$. The data are taken in a field of 10 kG; the data taken at 2 kG show little deviation. Measurements for two independently prepared samples are shown. The solid line is a theoretical fit to the data based on the models described in the text. Note that the logarithmic temperature scale emphasizes differences in the fit. The data shown in part a are calculated for a monomeric model; the μ values displayed have been calculated on that assumption. The data shown in part b are calculated for the dimeric model described in the text and the effective magnetic moments shown in part b are calculated assuming that the molecules behave as dimers.

ion are treated by a crystal field model in which the vanadium experiences a strong octahedral field which splits the 3d multiplet into a t_{2g} triplet and a higher energy e_g doublet. We ignore the doublet since it is much higher in energy. Lower symmetry components of the field (tetragonal and rhombic) will split the t_{2g} triplet into three singlet states (d_{xy}, d_{xz}, d_{yz}) which are mixed by spin–orbit coupling. This crystal field model is equivalent to the Griffith model[21] used to describe low-spin ferric systems. The magnetic moment of the vanadium electron then couples to the porphyrin cation radical. The Hamiltonian used for this model is

$$\mathcal{H} = V_{ax} + V_{rh} + \zeta\vec{l}\cdot\vec{s}_v - J(\vec{l} + 2\vec{s}_v)\cdot\vec{s}_r + \mu_B(\vec{l} + 2\vec{s}_v + 2\vec{s}_r)\cdot\vec{H}$$

and where V_{ax} and V_{rh} are the axial (tetragonal) and rhombic components of the crystal field, ζ is the spin–orbit coupling parameter, $\vec{l}$ is the vanadium electron orbital angular momentum vector, and $\vec{s}_v$ and $\vec{s}_r$ are the spins of the vanadyl electron and the porphyrin cation radical, respectively. We treat V_{ax}, V_{rh}, ζ, and J as adjustable parameters to best fit the observed magnetic susceptibility data. We note that an axially symmetric molecule (such as this molecule) should have $V_{rh} = 0$. With the above Hamiltonian, $J < 0$ corresponds to antiferromagnetic coupling of the spins and will result in a diamagnetic ground state, with

(21) Griffith, J. S. *Nature* **1957**, *180*, 30.

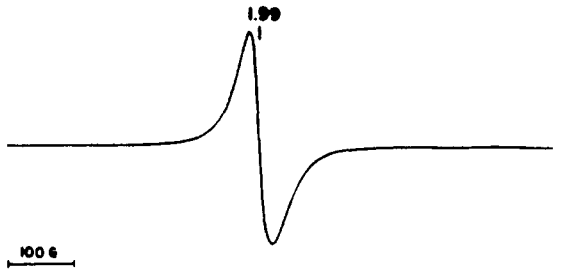

Figure 4. Solid-state (powder) EPR spectrum of $[VO(OH_2)(OEP^{\bullet})]SbCl_6$.

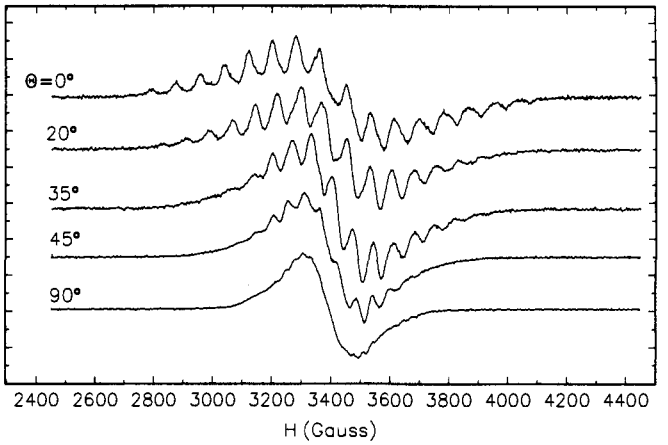

Figure 5. Single-crystal EPR spectra of $[VO(OH_2)(OEP^{\bullet})]SbCl_6$. The spectra were taken at 9.449 GHz, at a temperature of about 5 K. Several small crystals, which had the form of long narrow plates, were aligned on the EPR flat so that the long axes remained perpendicular to the magnetic field as the sample was rotated. Angles shown in the figure are rotations of the crystal relative to the magnetic field.

an excited state of total spin $S = 1$. For $J > 0$, the ground state will have $S = 1$, and this spin triplet will have a zero field splitting induced by the spin–orbit coupling. The magnetic data can be best fit using the parameters $V_{ax} = 57$ cm^{-1}, $\zeta = 114$ cm^{-1}, and $J = -14$ cm^{-1} and thus the two spin systems of the molecule are antiferromagnetically coupled. The agreement between the simulation and the experimental data is displayed in Figure 3a. However, this susceptibility model does not predict the observed EPR spectrum (vide infra) for $[VO(OH_2)(OEP^{\bullet})]SbCl_6$.

The solid-state (powder) EPR spectrum for the OEP complex shows a single, relatively broad line at $g = 1.99$ that is illustrated in Figure 4. The intensity of the powder EPR spectrum increases with temperature, an indication that the EPR transition must arise from an excited state. Solution-state EPR spectra for $[VO(OH_2)(OEP^{\bullet})]SbCl_6$ have extremely different spectra depending on temperature but are identical to those reported previously.[12,13] The *solution* EPR spectra at both high and low temperatures show vanadium hyperfine splitting. The room temperature spectrum (with eight lines) has been interpreted in terms of an intramolecular coupling process,[13] while the low-temperature spectrum (fifteen lines with $g_\parallel$ and $g_\perp$ branches) results from a vanadium–vanadium triplet as a consequence of forming a strongly coupled radical cation dimer.[12] Subsequently, we were able to obtain single-crystal EPR on $[VO(OH_2)(OEP^{\bullet})]SbCl_6$ which shows well-resolved angle-dependent vanadium hyperfine structure. In Figure 5 it can be seen that the hyperfine lines are not equal in intensity, but rather have intensity ratios of about 1:2:3:4:5:6:7:8:7:6:5:4:3:2:1. These intensity ratios are what one would expect for two coupled $I = {}^7/_2$ vanadium nuclei. We thus conclude that $[VO(OH_2)(OEP^{\bullet})]SbCl_6$ molecules couple magnetically in pairs in the solid state.

The second magnetic susceptibility model assumes that the $[VO(OH_2)(OEP^{\bullet})]SbCl_6$ molecules act as dimers in which there is intramolecular magnetic coupling between a $\vec{s}_v = {}^1/_2$ vanadyl

d-electron and a $\vec{s}_r = {}^1/_2$ cation radical, and at the same time intermolecular coupling between two cation radicals. The Hamiltonian that describes this model is

$$\mathcal{H} = -J_{v-r}(\vec{s}_v \cdot \vec{s}_r + \vec{s}'_v \cdot \vec{s}'_r) - J_{r-r}(\vec{s}_r \cdot \vec{s}'_r) + g\mu_B \vec{H} \cdot (\vec{s}_v + \vec{s}'_v + \vec{s}_r + \vec{s}'_r)$$

J_{v-r} and J_{r-r} describe the intra- and intermolecular magnetic coupling, respectively, and were varied to find the best fit to the susceptibility data. The best fit was obtained with the parameters $J_{v-r} = 63$ cm^{-1} (ferromagnetic) and $J_{r-r} = -139$ cm^{-1} (antiferromagnetic).

The above coupling model results in an EPR-silent $S_{total} = 0$ ground state, excited states having $S_{total} = 1$ at 7, 164, and 189 cm^{-1}, an excited state with $S_{total} = 2$ at 125 cm^{-1}, and a $S_{total} = 0$ state at 235 cm^{-1}. The $S = 1$ and 2 states should be EPR active, with absorption near $g = 2$. The fact that these EPR-active states are all excited states qualitatively explains the observed temperature-dependent EPR intensity.

Discussion

All spectroscopic data for [VO(OH$_2$)(OEP$^\bullet$)]SbCl$_6$ are consistent with its formulation as a π-cation radical complex. It exhibits the broad bands in the visible portion of the UV–vis spectra that are typical of a π-cation radical and also displays the strong, characteristic marker band in the infrared (at 1533 cm^{-1}) characteristic for a radical.[22] The unsplit Sb–Cl stretch suggests that there is no interaction between the cation and anion; this is confirmed for [VO(OH$_2$)(OEP$^\bullet$)]SbCl$_6$ by the structure determination.

The effective six-coordinate nature of [VO(OH$_2$)(OEP$^\bullet$)]SbCl$_6$ is shown by the results of the X-ray structure determination. The displacement of the vanadium atom from the mean plane of the 24-atom core, 0.46 Å in [VO(OH$_2$)(OEP$^\bullet$)]SbCl$_6$, is less than the average 0.52-Å displacement seen in the six neutral five-coordinate vanadyl porphyrin complexes of known structure.[23-26] More importantly, the 2.063(3) Å value for the average V–N$_p$ distance is significantly smaller than the average 2.102(6) Å value for neutral [VO(OEP)][26] or the 2.075 Å value for all the other five-coordinate complexes.[23-25] The V–N$_p$ distance thus confirms the significant effects of six-coordination. The sixth ligand, the axial water molecule, is apparently derived from residual water in solvent. Its coordination trans to the oxo ligand of the vanadyl ion is a bit surprising given the strong preference for five-coordination displayed by most vanadyl complexes. We note, however, that in our experience metallo π-cation derivatives display substantially enhanced affinity for aquo ligands relative to the ring neutral analogs, presumably because of the overall positive charge. Although the structure determination might be considered as evidence for a partially occupied sixth ligand, the reproducibility of the single-crystal and bulk preparations points to a significant role of the sixth ligand. (The preparation has been reproduced on several occasions as shown by spectroscopic measurements, reproducible magnetic susceptibility results, and unit-cell determinations.)

An interesting, if difficult, question concerns the possible changes in core bond lengths that result from oxidation of the ligand. We note that such changes in bond distance are expected to be small given the large number and complexity of the bonding molecular orbitals for the porphyrin core. Moreover, even if bond distance variations were occurring, their presence might well be obscured by positional (rotational) disorder of the porphyrin core in the crystal lattice which yields core parameters having higher apparent symmetry than that which actually exists.[27]

For several *meso*-tetraarylporphyrin derivatives,[3-6,28,29] no apparent pattern of bond distance variation has been observed. However, significant variations in bond distance were found for the novel OEP radical dimer [Zn(OH$_2$)(OEP$^\bullet$)]$_2$(ClO$_4$)$_2$, where the N–C$_a$ and C$_a$–C$_m$ (the bonds of the great inner 16-membered ring) were found to alternate in a long–short pattern.[7] A similar long–short pattern is found for [Fe(OEP$^\bullet$)(Cl)]$_2$(ClO$_4$)$_2$.[8] Moreover, the C$_a$–C$_b$ bonds are slightly longer than the normal value for neutral porphyrins. Bond distances in the core of [VO(OH$_2$)(OEP$^\bullet$)]SbCl$_6$ (Table 3) do not conform to the alternating pattern observed in the [Zn(OEP)] and [Fe(OEP)(Cl)] radical systems. Although we do not believe that an alternating bond distance pattern is present in [VO(OH$_2$)(OEP$^\bullet$)]SbCl$_6$, it is possible that it is obscured by rotational disorder. However, one averaged bond distance in the [VO(OH$_2$)(OEP$^\bullet$)]SbCl$_6$ core (Figure 2) displays a value analogous to the zinc and iron complexes[30] albeit not with absolute statistical significance.[32] The C$_a$–C$_b$ bond distances are 0.015–0.020 Å longer than normal[31] in both the vanadyl and zinc octaethylporphyrin derivatives. It is precisely these C$_a$–C$_b$ bonds that should be lengthened if the species has a predominantly a_{1u} ground state as has been assigned.[33] Most TPP radicals, on the other hand, are assigned an a_{2u} ground state and the C$_a$–C$_b$ bond distances are not expected, nor observed, to be significantly affected in this state.

The conformation of the porphinato core in [VO(OH$_2$)(OEP$^\bullet$)]SbCl$_6$ represents an S$_4$-ruffled type not previously observed for π-cation radical derivatives. The core conformations of porphyrin radicals previously studied have fallen into two main groups. The first group, comprised of the several four- and five-coordinate *tetraphenyl*porphyrin derivatives that form π–π dimers in the solid state, have nonplanar porphinato cores that are extremely S$_4$-ruffled.[34] We have noted elsewhere[4,6,35] that we believe that these extremely saddle-shaped porphyrin cores result from the distortions needed to alleviate the generally strong dimer-hindering effects of the peripheral phenyl groups. The second known group, much smaller in number, consists of five complexes[3,6-8] having essentially planar porphinato cores. We have previously noted[6,7] that the available evidence was inadequate to conclude that the porphyrin π-cation radicals had a particular conformational preference, in particular, the S$_4$-ruffled (saddle-shaped) core is not the intrinsic core conformation for the radicals. The

(22) Shimomura, E. T.; Phillippi, M. A.; Goff, H. M.; Scholz, W. F.; Reed, C. A. *J. Am. Chem. Soc.* **1981**, *103*, 6778.
(23) Petersen, R. C. *Acta Crystallogr., Sect. B* **1969**, *B25*, 2527.
(24) Miller, S. A.; Hambley, T. W.; Taylor, J. C. *Aust. J. Chem.* **1984**, *37*, 761.
(25) Drew, M. G. B.; Mitchell, P. C. H.; Scott, C. E. *Inorg. Chim. Acta* **1984**, *82*, 63.
(26) Molinaro, F. S.; Ibers, J. A. *Inorg. Chem.* **1976**, *15*, 2278.
(27) An imperfect parallel is given by the structures of the free base species and the problem of the location of the inner hydrogen atoms of the porphyrin.
(28) Spaulding, L. D.; Eller, P. G.; Bertrand, J. A.; Felton, R. H. *J. Am. Chem. Soc.* **1974**, *96*, 982.
(29) Barkigia, K. M.; Spaulding, L. D.; Fajer, J. *Inorg. Chem.* **1983**, *22*, 349.
(30) The averaged values for N–C$_a$, C$_a$–C$_m$, and C$_a$–C$_b$ in [Zn(OH$_2$)(OEP$^\bullet$)]$_2$(ClO$_4$)$_2$ are 1.364, 1.394, and 1.467(2) Å, respectively.[7] Analogous values for [Fe(OEP$^\bullet$)(Cl)]$_2$(ClO$_4$)$_2$ are 1.374, 1.389, and 1.453(7) Å.[8] Note that in both species there are two groups of bond distances (long and short) for N–C$_a$ and C$_a$–C$_m$.
(31) The averaged values for N–C$_a$, C$_a$–C$_m$, and C$_a$–C$_b$ in VO(OEP) are 1.379(5), 1.387(7), and 1.447(6) Å, respectively,[26] which are at least quite close to normal values for neutral porphyrin derivatives.
(32) We point out that this particular bond pattern would be unaffected by the presence of rotational disorder.
(33) Sandusky, P. O.; Salehi, A.; Chang, C. K.; Babcock, G. T. *J. Am. Chem. Soc.* **1989**, *111*, 6437. Czernuszewicz, R. S.; Macor, K. A.; Li, X.-Y.; Kincaid, J. R.; Spiro, T. G. *J. Am. Chem. Soc.* **1989**, *111*, 3860.
(34) There are two types of idealized S$_4$(D_{2d})-ruffled core conformations in porphyrin complexes. These differ by a rotation of the symmetry elements by 45° about the axis normal to the plane. Thus, the methine carbon atoms (C$_m$) are either alternatively above and below the porphyrin plane or on the mean porphyrin plane. The former conformation is more common although it is observed in the present case for the first time for a π-cation radical derivative. The latter has a saddle-shaped surface described for the π-cation species in which both β-carbon atoms of individual pyrrole rings are alternatively displaced above or below the mean plane of the 24-atom core. The displacements of the β-carbon atoms in these saddle-shaped radicals are substantial larger than normal and are frequently greater than ±0.60 Å.
(35) Scheidt, W. R.; Lee, Y. J. *Struct. Bonding (Berlin)* **1987**, *64*, 1.

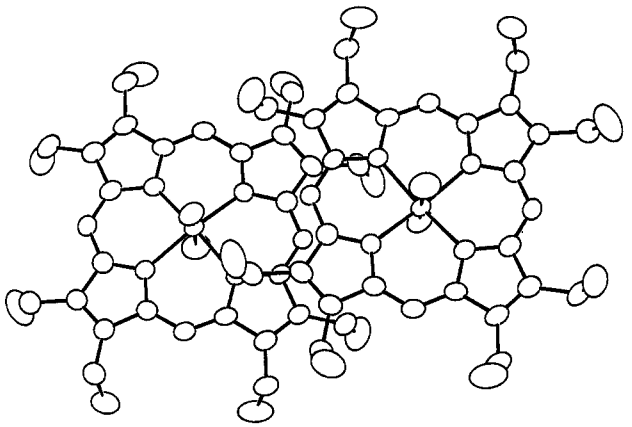

Figure 6. Diagram illustrating a possible radical–radical spin coupling path. The two molecules are related by an inversion center. The two porphyrin planes are parallel to each other and to the plane of the drawing.

conformational data for $[VO(OH_2)(OEP^{\bullet})]SbCl_6$ now allow us to add that it appears likely that the π-cations are as conformationally adaptable as neutral porphyrin derivatives.

Earlier (solution) EPR studies[10] of the vanadyl octaethylporphyrin radical cation had been interpreted in terms of a monomeric, triplet state. However, the observed nonlinearity and decrease of the (solid-state) magnetic moment with decreasing temperature (Figure 3) make it obvious that an $S = 1$ state cannot be the ground state for the present material. The falloff of the moment with decreasing temperature must result from a lower multiplicity ground state with a higher multiplicity excited state(s). Thus, the magnetic data for $[VO(OH_2)(OEP^{\bullet})]SbCl_6$ clearly require an overall antiferromagnetic coupling scheme. The six-coordinate nature of the complex led us to attempt to fit the magnetic data with an intramolecular coupling scheme between the unpaired electrons on the vanadyl ion and the porphyrin radical. However, the temperature-dependent rate of change is inconsistent with a simple Bleaney–Bowers singlet–triplet model.[36] As described in the Results, we did find a crystal-field model that fits the observed magnetic data well (Figure 3a). Still, the fact that this model does not predict the observed powder EPR signal ($g \sim 1.99$) was viewed as a serious deficiency and led us to examine the problem in further detail.

Two additional EPR experiments were most informative. Quantitative studies showed that indeed the EPR intensity increased with increasing temperature and the single-crystal EPR spectrum showed vanadium hyperfine structure which clearly suggested a vanadium–vanadium interaction. We then investigated dimer magnetic susceptibility models. We started with a model that assumes intramolecular coupling between the vanadyl and the porphyrin radical and intermolecular coupling between the porphyrin radicals. To fit the susceptibility data with this model, it was necessary to have ferromagnetic coupling between the vanadyl and radical spins within a molecule and antiferromagnetic coupling between molecules. Quite acceptable fits to the experimental susceptibility data result (see Figure 3b). Significantly, this model provides a qualitatively acceptable prediction of the observed EPR properties (both the g-value and temperature dependence of signal intensity). Although inclusion of intermolecular vanadium–vanadium coupling into the model might improve the fit at high temperatures, this is not warranted. Decreased signal-to-noise ratios and the inherent uncertainty in the diamagnetic correction diminish the quality of the data as the temperature increases.

While the closest V···V separations of ~7.5 and 7.9 Å would seem to be more consistent with noninteracting molecules, we have identified a plausible intermolecular spin-coupling path in the solid-state structure. Figure 6 is an ORTEP diagram of the two closest $[VO(OH_2)(OEP^{\bullet})]SbCl_6$ molecules. The two molecules are related by an inversion center so that the porphinato planes are parallel to each other and, in this diagram, the porphinato planes are parallel to the plane of the paper. The perpendicular separation between the two planes is 3.30 Å. As is evident in the diagram, the $[VO(OH_2)(OEP^{\bullet})]SbCl_6$ molecule has no direct overlap with its neighbor. Nonetheless, there is an interesting edge-to-edge interaction visible in the diagram. Note the saw-tooth edge-to-edge "docking" that leads to a total of six close C···C interring distances. These C···C distances range from 3.56 to 3.67 Å.[37] Moreover, since the π-cation radical of $[VO(OH_2)(OEP^{\bullet})]SbCl_6$ is of the a_{1u} type, four of the six atom–atom pairs involved have atoms in both rings with large unpaired spin density.[38] Thus this structurally suggested path has the correct symmetry for a significant radical–radical spin-coupling interaction.

It is to be emphasized that the proposed solid-state coupling mechanism for the radical and vanadyl spins is distinctly different from either coupling mechanism deduced from the solution-state EPR spectra of the $[VO(OEP^{\bullet})]^+$ system. At room temperature (fluid solution), $[VO(OEP^{\bullet})]^+$ displays an eight-line spectrum with inverted line widths[13] that has been interpreted as an intramolecular, $S = 1$ coupled system. The coordination number of the room temperature species is unknown; either five- or six-coordination could be consistent with the magnetic properties. In frozen solution (80 K), the $[VO(OEP^{\bullet})]^+$ system displays a fifteen-line spectrum with $g_{\parallel}$ and $g_{\perp}$ branches that can be interpreted in terms of an $S = 1$ dimer.[12] A detailed fit requires a V–V separation of 4.7 Å for the frozen solution dimer, much shorter than the 7.45 Å observed in the present solid-state case. The model also requires stronger radical–radical coupling and weak V–V coupling. Neither of these conditions is consistent with the solid-state susceptibility nor the powder or single-crystal EPR properties from isolated, crystalline $[VO(OH_2)(OEP^{\bullet})]SbCl_6$ show both temperature-dependent types of solution EPR spectra and our observed spectra are indistinguishable from the published spectra.[12,13] The EPR-calculated 4.7-Å distance for the frozen solution dimer[12] is just slightly longer than expected if the compound had the two rings completely overlapped as in the crystallographically characterized $[Zn(OH_2)(OEP^{\bullet})]_2^{2+}$ dimer complex.[7] Thus it seems clear that in frozen solution $[VO(OH_2)(OEP^{\bullet})]SbCl_6$ must lose the coordinated water molecule to form a more tightly coupled dimer:

$$2[VO(OH_2)(OEP^{\bullet})]^+ (RT) \rightleftharpoons [VO(OEP^{\bullet})]_2^{2+} + 2H_2O (LT)$$

The reasons for the difference in interring interactions in the two states are not entirely obvious. The temperature-dependent solution differences must result from the fact that the solution dimerization equilibrium is relatively weak with a concomitant small equilibrium constant and thus the strongly coupled dimer is only accessible at low temperatures. It is then a natural presumption that the strongly coupled dimer does not crystallize because its room temperature concentration is too low or *that* its solubility is higher than that of the aquo monomer.

As noted in the Introduction, the porphyrin core conformation in π-cation radical derivatives controls whether a paramagnetic metal ion exhibits intramolecular ferro- or antiferromagnetic spin coupling. The structural and magnetic characterization of $[VO(OH_2)(OEP^{\bullet})]SbCl_6$ now allows us to define some additional

(36) Bleaney, B.; Bowers, K. D. *Proc. R. Soc. London* **1952**, *A214*, 451.

(37) An approximate calculation using the radial extent of an H_{2p_z} orbital gives $\langle z^2 \rangle^{1/2}$ of 2.2 Å. There thus appears to be adequate overlap for coupling.

(38) Gouterman, M. In *The Porphyrins*; Dolphin, D., Ed.; Academic Press: New York, 1978; Vol. III, Chapter 1. In an a_{1u} radical, meso-carbon the atoms do not have significant unpaired electron density; the C_a and C_b atoms do.

structural/coupling correlation principles. The combination of solution and solid-state characterization of $[VO(OEP^{\bullet})]^{+}$ derivatives demonstrates that as the intermolecular interactions are changed, substantial differences in the nature and magnitude of spin coupling arise. In the absence of intermolecular interactions, $[VO(OEP^{\bullet})]^{+}$ displays only an intramolecular ferromagnetic interaction that follows previous porphyrin core conformation/coupling paradigms. The solution dimer appears to have a strongly overlapped pair of porphyrin rings that are almost certainly analogous to the three structurally characterized dimers.[7,8] The two radical spins strongly couple antiferromagnetically in all three of these cases as well as in the vanadyl derivative. The present solid-state system represents a new structural type, not previously recognized,[35] where the two porphyrin rings have no significant interring overlap but which the single-crystal EPR spectrum clearly shows must have an intermolecular coupling path. Structural studies suggest that this is an edge-to-edge interaction. What is perhaps most surprising is the relatively large magnitude ($J_{\pi-\pi} = -139$ cm^{-1}) of the interring radical coupling as deduced from the bulk susceptibility fit. Continued studies of intermolecular coupling interactions as the ring–ring overlaps are modulated are in progress.

Acknowledgment. This work was supported by the National Institutes of Health Grants GM-38401 (W.R.S.), GM-48513 (C.E.S.), DK-31038 (F.A.W.), and GM-23851 (C.A.R.).

Note Added in Proof: The line widths of the single crystal and solid state (microcrystalline) EPR spectra are consistent. Note that these spectra were measured at different temperatures. An analysis of A tensor values for the single-crystal experiments leads to the following probable limits: $A_{\parallel}/g_{\beta}$ is ~82 G and $A_{\perp}/g_{\beta}$ is ~25 G. These are typical values for vanadium(IV): Pilbrow, J. B. *Transition Ion Electron Paramagnetic Resonance*; Oxford University Press: New York, 1990.

Supplementary Material Available: Table S1, complete crystallographic details, Table S2, anisotropic thermal parameters, and Table S3, fixed hydrogen atom positions for $[VO(OH_2)(OEP^{\bullet})]SbCl_6$ (5 pages); listings (×10) of the observed and calculated structure amplitudes of $[VO(OH_2)(OEP^{\bullet})]SbCl_6$ (16 pages). This material is contained in many libraries on microfiche, immediately follows this article in the microfilm version of the journal, and can be ordered from the ACS; see any current masthead page for ordering information.